Radiation Protection Dosimetry (2021), pp. 1–9 doi:10.1093/rpd/ncaa218

DEVELOPMENT OF A NEUTRON DOSIMETRY SYSTEM BASED ON DOUBLE SELF-ACTIVATED CsI DETECTORS FOR MEDICAL LINAC ENVIRONMENTS

Yumika Hanada [1,*], Akihiro Nohtomi[1], Junichi Fukunaga[2] and Yoshiyuki Shioyama[3]
[1]Department of Health Sciences, Kyushu University, 3-1-1 Maidashi, Higashi-ku, Fukuoka 812-8582, Japan
[2]Department of Radiology, Kyushu University Hospital, 3-1-1 Maidashi, Higashi-ku, Fukuoka 812-8582, Japan
[3]Department of Radiology Informatics and Network, Graduate School of Medical Sciences, Kyushu University, 3-1-1 Maidashi, Higashi-ku, Fukuoka 812-8582, Japan

*Corresponding author: yumika.hanada@gmail.com

Received 1 August 2020; revised 31 October 2020; editorial decision 17 November 2020; accepted 17 November 2020

In the present study, by using double self-activated CsI detectors, the development of a neutron dosemeter system whose response indicates better agreement with the International Commission on Radiological Protection-74 rem-response was carried out to simply evaluate the neutron dose with high accuracy. The present double neutron dosemeter system, using a slow-neutron dosemeter (thermal to 10 keV) and a fast-neutron dosemeter (above 10 keV), consists of CsI scintillators wrapped with two types of neutron energy filtering materials: polyethylene and B_4C silicon rubber. After optimization of each filter thickness, to confirm the validity of our method, the neutron ambient dose equivalents under several operating conditions of medical linear accelerators (Linacs) were evaluated using a Monte Carlo simulation and an experiment with the present dosemeter. From these results, the present dosimetry system has enabled a more accurate neutron dose evaluation than our conventional dosemeter, and the present dosemeter was suitable for the neutron dosimetry for 10 MV Linac environments.

INTRODUCTION

Nowadays, high-precision X-ray therapy such as intensity-modulated radiotherapy and volumetric-modulated arc therapy, which delivers a high dose to the tumor while minimizing the dose to adjacent normal tissue, has been realized through the technological innovation[1]. However, in high-energy photon beams (greater than about 8 MeV), there is a disadvantage in that undesirable photoneutrons are generated from high-Z materials in the medical linear accelerator (Linac) head, and such neutrons have a high biological effectiveness, which causes the risk of secondary cancer[2]. In addition, the amount of the neutron generation is different depending on the treatment plans and Linac machines. Therefore, it is preferable to evaluate the photoneutron dose for each patient who received radiotherapy.

In our previous studies, we have proposed a novel neutron detection method that uses the self-activation of an iodine-containing scintillator such as a CsI scintillator[3]. Applying this method, Kakino *et al.*[4] and Nohtomi *et al.*[5] estimated the neutron fluence energy spectrum by unfolding based on the three-group approximation and evaluated the neutron ambient dose equivalent. Although a precise neutron dose evaluation is possible by the three-group approximation method, it is not suitable for daily neutron monitoring around medical Linacs because complicated and time-consuming procedures, such as four-time number of measurements for different conditions, are required. To evaluate simply the neutron ambient dose equivalent around medical Linacs, Ueki *et al.*[6] developed a neutron dosemeter by applying the neutron rem-counter technique[7] to the self-activation method. By using the neutron dosemeter, one can directly read the neutron ambient dose equivalent through a single measurement. However, there was about a 50% disagreement in the neutron dose between the value evaluated by the dosemeter and the value evaluated by the three-group approximation method[8] under the same conditions. As the reason for such a large disagreement, the response of the dosemeter indicated a large disagreement with the International Commission on Radiological Protection (ICRP)-74 rem-response[9]. Hence, the dosemeter using a single CsI scintillator has a limitation in matching the responses to the ICRP-74 rem-response.

In the present study, by using double self-activated CsI detectors, a development of a neutron dosemeter system whose response indicates better agreement with the ICRP-74 rem-response was carried out to simply evaluate the neutron ambient dose equivalents with a high accuracy. First, the neutron energy filters

used to cover each CsI scintillator were optimized for approaching the response of the present dosemeter to the ICRP-74 rem-response. The responses of the present dosemeter were checked using a Monte Carlo simulation, and we determined an optimum structure design. Next, to confirm the validity of the present method, the neutron ambient dose equivalents were evaluated by the present dosemeter under various Linac conditions through a Monte Carlo simulation and an experiment.

MATERIALS AND METHODS

Principle of $H^*(10)$ evaluation method using double self-activated CsI detectors

In the present neutron dose estimation method, the neutron ambient dose equivalent ($H^*(10)$) (μSv h^{-1}) is evaluated by adding a slow-neutron dose (H_s) from thermal to 10 keV and a fast-neutron dose (H_f) of above 10 keV. Each dose component is measured by a slow-neutron dosemeter and a fast-neutron dosemeter, respectively. Then, $H^*(10)$ is expressed as Equation (1),

$$H^*(10) = H_s + H_f = aA_s + bA_f, \tag{1}$$

where A_s and A_f are the saturated activities (Bq) of ^{128}I generated inside the CsI scintillators for slow- and fast-dosemeters, respectively. The conversion factors a and b are obtained by the following:

$$a = \frac{\int_{\text{thermal}}^{10\text{keV}} h_{10}^*(E)\phi(E)\mathrm{d}E}{\int_{\text{thermal}}^{10\text{keV}} R_s(E)\phi(E)\mathrm{d}E} = \frac{H_s}{A_s}, \tag{2}$$

$$b = \frac{\int_{10\text{keV}} h_{10}^*(E)\phi(E)\mathrm{d}E}{\int_{10\text{keV}} R_f(E)\phi(E)\mathrm{d}E} = \frac{H_f}{A_f}, \tag{3}$$

where $\phi(E)$ is the neutron fluence rate (n cm^{-2} s^{-1}), $h_{10}^*(E)$ is the ICRP-74 rem-response (μSv cm^2) and $R_f(E)$ and $R_s(E)$ are the response of the slow- and fast-neutron dosemeters (cm^2), respectively. To realize this evaluation method, it is necessary to bring the dosemeter response close to the ICRP-74 rem-response.

Optimization of design of the neutron dosemeter using double self-activated CsI detectors

We adopted the commercially available gamma radiation detection module C12137 made by Hamamatsu Photonics[10] as the CsI scintillator applied to the self-activation method. The module contains a 13 mm × 13 mm × 20 mm CsI(Tl) scintillator crystal and a photosensor Multi-Pixel Photon Counter (MPPC). By connecting it to the USB port of the personal computer, the pulse height distribution can be easily read out. When this module is applied to the self-activation method, after the termination of neutron irradiation to the module, the beta rays from ^{128}I are measured, which are generated inside the CsI scintillator itself through the capture reaction ^{127}I(n, γ)^{128}I.

The cross-section of ^{127}I(n, γ)^{128}I decreases monotonously with the increase in neutron energy by the 1/v law. Therefore, to approach the ICRP-74 rem-response, it was necessary to modify the response curve by using neutron energy filters. For the neutron energy filters, polyethylene (P.E.) for the neutron moderator and B_4C 50 wt% silicon rubber (B_4C) for the thermal neutron absorber were adopted. P.E. was selected as the neutron energy filter for the slow-neutron dosemeter to bring the dosemeter response close to the ICRP-74 rem-response in the slow-neutron region with a flat response. For the neutron energy filters of the fast-neutron dosemeter, P.E. and B_4C were used as the outer and inner layers, respectively, to bring the dosemeter response close to the ICRP-74 rem-response in the fast-neutron region, which is characterized by a rapidly increasing curve up to 1 MeV. In addition, the cylindrical cavity space was arranged at the center of each neutron filter for setting the C12137.

The response of the dosemeter with a CsI scintillator equipped with various filters was calculated by a [T-Yield] tally of the Particle and Heavy Ion Transport code System (PHITS) version 3.06 as a Monte Carlo simulation[11]. Next, the optimum thicknesses of each neutron filter were determined through trial and error on the basis of the residual sum of square (RSS) between the ICRP-74 rem-response and the response of the dosemeter. The RSS is a measure of the discrepancy between the data and an estimation model, and a smaller RSS indicates a tight model fit to the data. In this case, the RSS was calculated by using following Equation (4):

$$\mathrm{RSS} = \sum_i \{h^*(E_i)_{\text{ICRP}} - R(E_i)_{\text{cal.}}\}^2, \tag{4}$$

where $h^*(E_i)_{\text{ICRP}}$ indicates the ICRP-74 rem-response with the meaning of the estimation model and $R(E_i)_{\text{cal.}}$ indicates the response calculated by PHITS with the meaning of the data. For the slow-neutron dosemeter, the RSS was calculated by changing the thickness of the P.E. from 1.75 to 2.0 cm. For the fast-neutron dosemeter, the response of the fast-neutron dosemeter was calculated by changing the P.E. thickness to between ±2 and 7 cm, which was adopted for the thickness of the outer P.E. of our conventional dosemeter by Ueki *et al.*[6], and a B_4C thickness from 1 to 10 mm. Then, the response was closer to the ICRP-74 rem-response when the

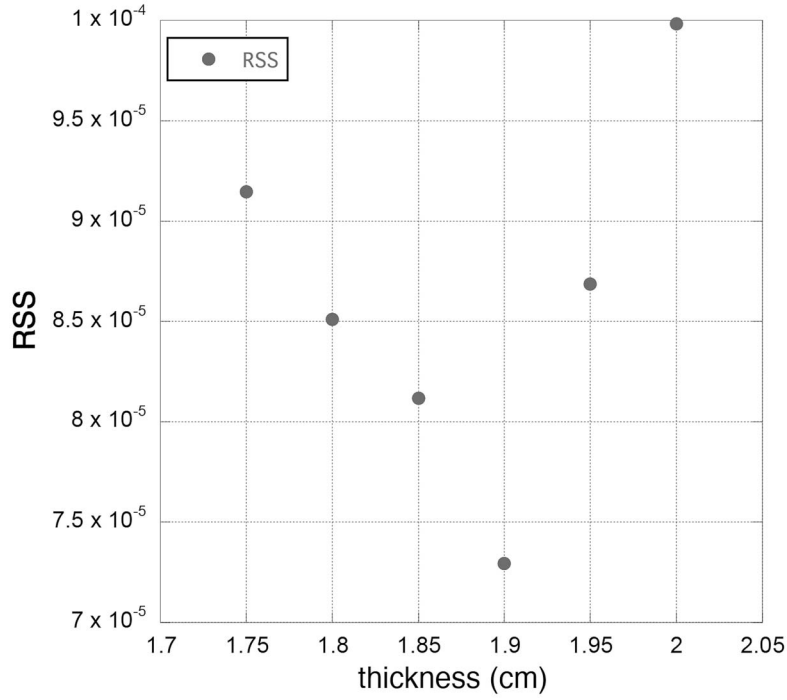

Figure 1: The RSS for the slow-neutron dosemeter.

total thickness was 7.5 cm, and the RSS was finally calculated by changing each thickness of the P.E. and the B_4C while keeping the total thickness at 7.5 cm.

As a result, the RSS reached a minimum value for the slow-neutron dosemeter when the thickness of the P.E. was 1.9 cm (Figure 1). For the fast-neutron dosemeter, the RSS reached the minimum value when the thicknesses of P.E. and B_4C were 7.0 and 0.5 cm, respectively (Figure 2). Figure 3 shows the structures of slow- and fast-neutron dosemeter. The overall size of the slow-neutron dosemeter is 9.8 cm in diameter and 12.9 cm in length, and the overall size of fast-neutron dosemeter is 21.0 cm in diameter and 18.5 cm in length. A cavity space is arranged at the center of both filter structures for the insertion of C12137, whose size is 6.0 cm in diameter and 11.0 cm in length.

The responses of slow- and fast-neutron dosemeters are shown in Figure 4. The rather good agreement between the responses and the ICRP-74 rem-responses in a wide energy range from thermal to 3 MeV neutrons for each energy region was confirmed, except the epithermal region. Such agreement is suitable for neutron measurements around 10 MV medical Linacs, which is the most common acceleration voltage in Japan[12], because there are almost no neutrons of over 1 MeV[13]. Figure 5 shows the total response curve obtained by adding the response of the present slow- and fast-neutron dosemeter in Figure 4. The response curve of our conventional neutron dosemeter is also displayed for comparison, which was designed by Ueki *et al.*[6] using a single detector with the neutron rem-counter technique concept. Compared with the response of the slow-neutron dosemeter in the epithermal region of Figure 4, the total response curve was farther from the ICRP-74 rem-response. This is because the response of the fast-neutron dosemeter is added to the response of the slow-neutron dosemeter in this region. However, in this figure, a clear improvement of the present dosemeter response can be seen, particularly in the thermal neutron region, based on the comparison with that of our conventional neutron dosemeter. In addition, the response in the fast-neutron region, where the ICRP-74 rem-response shows a high value, is closely matched up to 3 MeV. Thus, it may be suitable for an evaluation of the ambient dose equivalent of neutrons whose energy ranges from thermal to fast-neutron region around Linacs.

The angular dependences of the present neutron dosemeter responses were calculated by irradiating the neutron beam from 0, 45 and 90° (Figure 6) in the PHITS simulation. The results of the angular dependences are shown in Tables 1 and 2. The angular

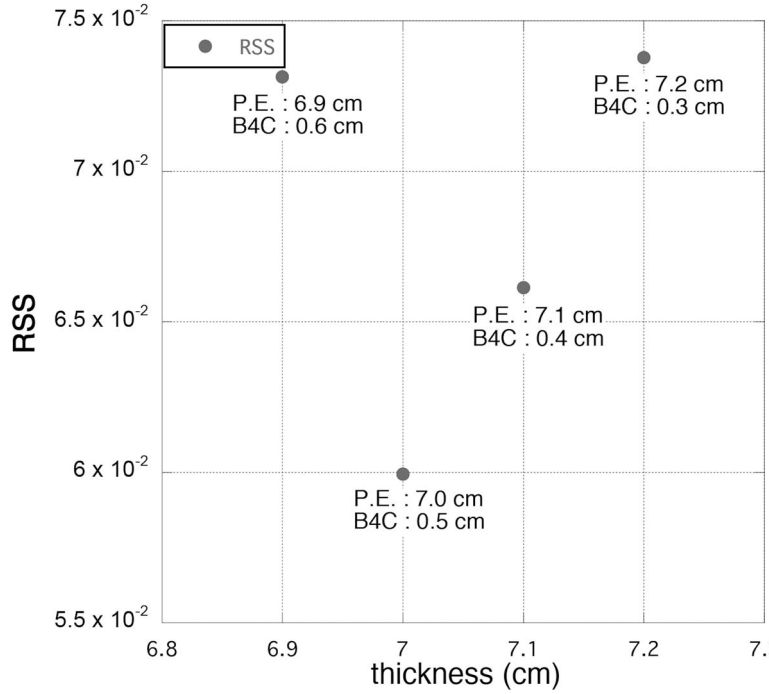

Figure 2: The RSS for the fast-neutron dosemeter.

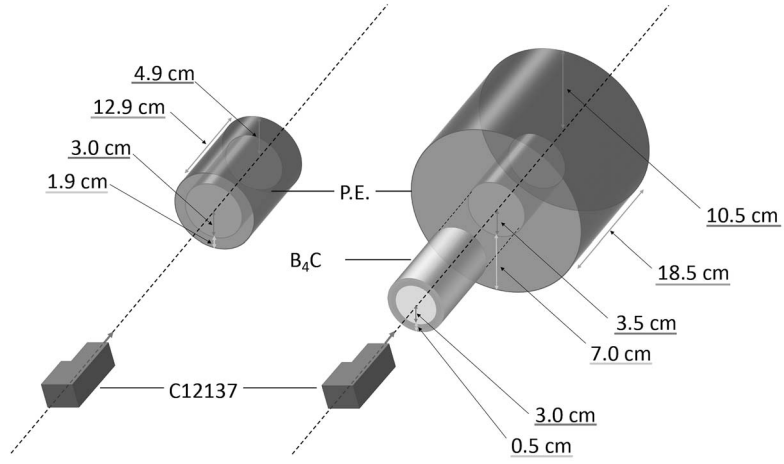

Figure 3: Schematics of the designed slow- and fast-neutron dosemeter.

dependences of each dosemeter are expressed as the ratios normalized by the response irradiated from 90° for each neutron energy. As a result, the deviation of the 0° response from a 90° response was within approximately ±15%, whereas the deviation of the 45° response from a 90° response was rather large. Therefore, when deriving a conversion factor, it is necessary to carefully consider the angular dependence of the response. In the following section, the deviation of the conversion factor is explained in detail.

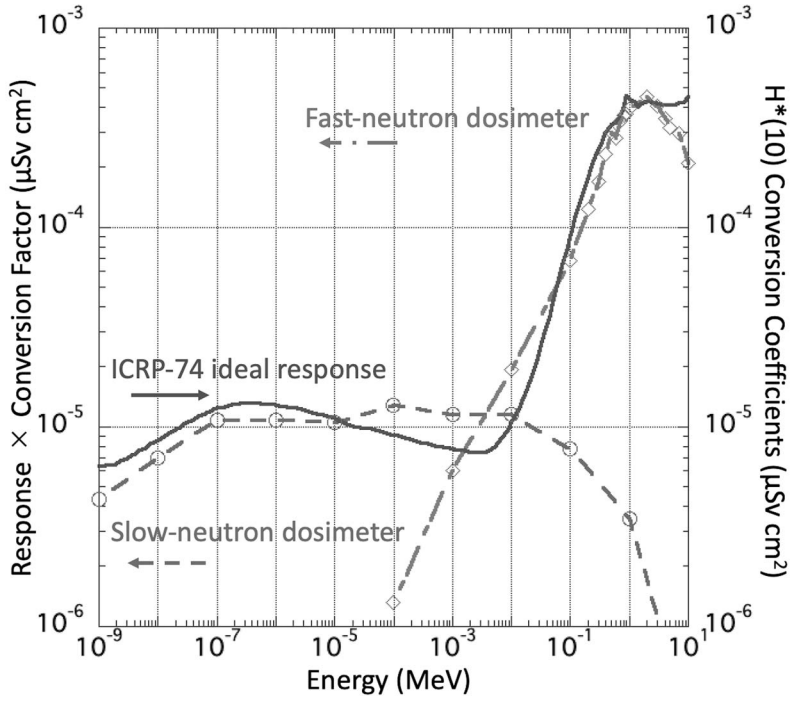

Figure 4: A comparison between the ICRP-74 ideal rem-response and calculated responses of the optimized slow- and fast-neutron dosemeter.

Table 1. Angular dependence of the response of the slow-neutron dosemeter

Neutron energy (MeV)	Direction θ (degree)		
	0	90	45
1.0×10^{-9}	0.985	1	1.72
1.0×10^{-8}	1.06	1	1.46
1.0×10^{-7}	1.01	1	1.43
1.0×10^{-6}	1.02	1	1.66
1.0×10^{-5}	0.964	1	1.73
1.0×10^{-4}	0.965	1	1.49
1.0×10^{-3}	1.04	1	1.76
1.0×10^{-2}	0.889	1	1.07

Table 2. Angular dependence of the response of the fast-neutron dosemeter

Neutron energy (MeV)	Direction θ (degree)		
	0	90	45
1.0×10^{-3}	1.11	1	1.06
1.0×10^{-2}	0.962	1	1.08
1.0×10^{-1}	1.12	1	1.25
1.0×10^{0}	0.89	1	1.25
3.0×10^{0}	1.06	1	1.39
5.0×10^{0}	1.15	1	1.43
7.0×10^{0}	0.974	1	1.29
1.0×10^{1}	1.04	1	1.46

Derivation of conversion factors

Typical information of appropriate neutron fluence rate spectra is required in the low-energy neutron field (thermal to 10 keV) and the high-energy neutron field (above 10 keV) for deriving conversion factors a and b by using Equations (2) and (3). Accordingly, we referred to the spectrum and the neutron ambient dose equivalents H_s at the thermal neutron calibration field[14] and the spectrum and the neutron ambient dose equivalents H_f at the fast-neutron calibration field[15] in the Japan Atomic Energy Research Institute. In the PHITS simulation, to obtain the denominator components A_s and A_f in Equations (2) and (3), neutron beams having the spectra at the thermal and the fast-neutron calibration fields were irradiated from 0, 45 and 90° to slow- and fast-neutron dosemeters, respectively. And each saturated activity of iodine in CsI scintillator

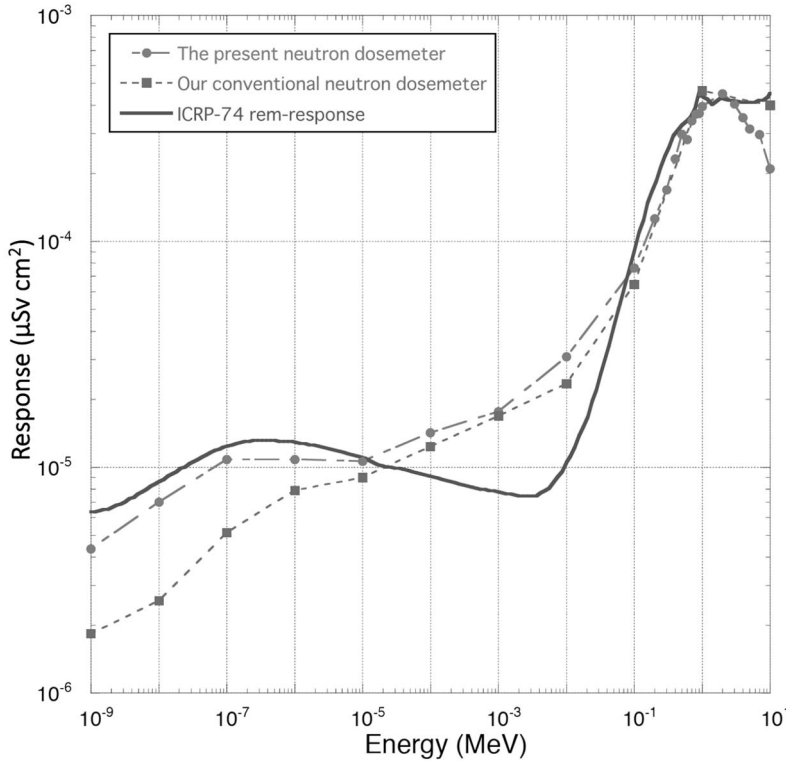

Figure 5: Comparison between the total response adding the response of the present slow- and fast- neutron dosemeter and the response of our conventional neutron dosemeter designed by Ueki *et al.*[6].

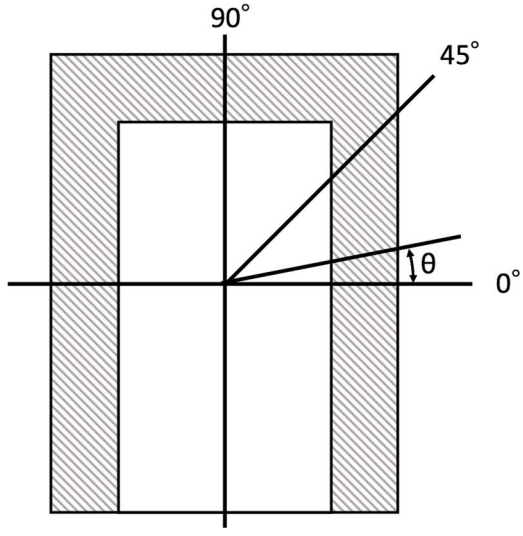

Figure 6: Neutron irradiation from 0, 45 and 90° direction in PHITS simulation.

was calculated. Conversion factors were derived by dividing H_s and H_f by A_s and A_f, respectively, as shown in Equations (2) and (3). Furthermore, these conversion factors calculated by PHITS simulation from each angle were averaged, and the conversion factors a and b were finally derived as follows:

$$a = 0.303 \pm 0.00974 \ \left(\mu\text{Sv Bq}^{-1}\ \text{h}^{-1}\right), \tag{5}$$

$$b = 62.5 \pm 2.11 \ \left(\mu\text{Sv Bq}^{-1}\ \text{h}^{-1}\right). \tag{6}$$

In the present neutron dosemeter, the neutron ambient dose equivalents are calculated using Equations (1), (5) and (6).

CONFIRMATION OF THE VALIDITY OF THE PRESENT METHOD

The neutron ambient dose equivalents were evaluated by the present neutron dosemeter at Linacs at various acceleration voltages. Simulation tests were conducted at Linacs with an accelerator voltage of

Table 3. Comparison of the neutron ambient dose equivalents evaluated by Domingo *et al.*[16] ($H^*(10)_{ref.}$) and the three-group approximation method[4] ($H^*(10)_{thr.}$) and the present method ($H^*(10)_{sim.}$)

Linac field (Linac conditions)	$H^*(10)_{ref.}$ (mSv Gy_x^{-1})	$H^*(10)_{thr.}$ (mSv Gy_x^{-1})	$H^*(10)_{sim.}$ (mSv Gy_x^{-1})	$\varepsilon_{thr.}$	$\varepsilon_{sim.}$
Ramón y Cajal (Elekta, 15 MV)	0.403	0.448	0.360	0.111	−0.106
Puerta de Hierro (Varian, 15 MV)	0.769	0.877	0.647	0.140	−0.159
Sevilla (Siemens, 15 MV)	0.532	0.586	0.442	0.102	−0.170
Valencia (Siemens, 18 MV)	0.595	0.621	0.494	0.0437	−0.169
Heidelberg (Siemens, 23 MV)	1.846	2.14	1.59	0.159	−0.137

$\varepsilon_{thr.}$ is relative error between $H^*(10)_{ref.}$ and $H^*(10)_{thr.}$ $\varepsilon_{sim.}$ is relative error between $H^*(10)_{ref.}$ and $H^*(10)_{sim.}$

above 15 MV. An experiment was conducted at a 10 MV Linac.

Simulation tests at Linacs with accelerator voltage of above 15 MV

The neutron ambient dose equivalents $H^*(10)_{ref.}$ measured under five medical Linac conditions reported by Domingo *et al.*[16] were compared with the neutron ambient dose equivalents $H^*(10)_{sim.}$ evaluated by the present neutron dosemeter with PHITS under the same conditions. The neutron beams with the energy spectra reported by Domingo *et al.*[16] were irradiated toward slow- and fast-neutron dosemeters in the 90° direction (Figure 6), and each estimated saturated activity was substituted into Equation (1) to evaluate $H^*(10)_{sim.}$

As a result, $H^*(10)_{ref.}$ and $H^*(10)_{sim.}$ are summarized in Table 3 with the neutron ambient dose equivalents $H^*(10)_{thr.}$ obtained by the three-group approximation method[4] simulated under the same conditions as in the present study. The values of $\varepsilon_{thr.}$ and $\varepsilon_{sim.}$ in Table 3 express the relative errors of $H^*(10)_{thr.}$ and $H^*(10)_{sim.}$ to $H^*(10)_{ref.}$, respectively. It is believed that the present dosemeter will underestimate the neutron dose because all values of $\varepsilon_{sim.}$ are negative. This underestimation is, as mentioned above, due to its disagreement between the ICRP-74 rem-response and the response of the present dosemeter in the neutron energy region at above 3 MeV. The acceleration voltage at five medical Linacs reported by Domingo *et al.*[16] was above 15 MV, and there is a non-negligible dose contribution from neutrons at above 3 MeV under such conditions. Consequently, it is assumed that the neutron dose evaluated by the present dosemeter was underestimated. By contrast, overall, the values of $\varepsilon_{sim.}$ were lower than ±17%, and the values of $\varepsilon_{thr.}$ were lower than ±16%. These results indicate that the present dosemeter was able to evaluate the neutron dose with a precision similar to that of the three-group approximation method in spite of the decreasing the number of measurements.

Figure 7: The present slow-neutron dosemeter and fast-neutron dosemeter.

Experiment at a medical Linac

We manufactured a finally designed double neutron dosemeter system (Figure 7) and conducted a performance test at a 10 MV medical Linac (Varian TrueBeam) at Kyushu University Hospital. To compare with the value evaluated in our previous studies[4,6], the test was conducted under the same conditions as in our previous studies, i.e. a field size of 40 cm × 9 cm and a photon dose rate of 3 Gy min^{-1} at the isocenter. Each neutron dosemeter was arranged so that the CsI scintillator in the dosemeter was set at 30 cm from the isocenter (Figure 8). After termination of the 30 min irradiation, the pulse height spectra were recorded for each C12137 every 1 min. We obtained a slow-neutron dose H_s and a fast-neutron dose H_f by multiplying the conversion factors a and b and each saturated activity estimated using the fitting process[17] with the decay curve of the counting rates. Finally, the neutron ambient dose equivalent $H^*(10)$ was evaluated by Equation (1).

The evaluated values of H_s and H_f were 5.87 ± 0.189 and 63.9 ± 2.16 (mSv Gy^{-1}), respectively. The final evaluation value of $H^*(10)$ was 6.97 ± 2.17

Table 4. Comparison of $H^*(10)$ at the 10 MV medical Linac evaluated by the three-group approximation method and our conventional dosemeter and the present method

	$H^*(10)_{thr.}$ (mSv Gy_X^{-1})	$H^*(10)_{con.}$ (mSv Gy_X^{-1})	$H^*(10)_{exp.}$ (mSv Gy_X^{-1})	$\varepsilon_{con.}$	$\varepsilon_{exp.}$
Varian TrueBeam	54.3	81.1 ± 7.13	69.7 ± 2.17	0.493	0.284

$H^*(10)_{thr.}$ and $H^*(10)_{con.}$ are evaluated by the three-group approximation method and our conventional dosemeter, respectively. $H^*(10)_{exp.}$ is evaluated by the present neutron dosemeter.

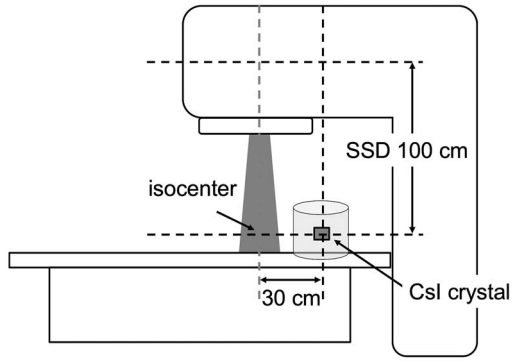

Figure 8: Schematic layout of the performance test at the 10 MV medical Linac.

(μSv/Gy), which is expressed as $H^*(10)_{exp.}$ below. The present neutron ambient dose equivalent $H^*(10)_{exp.}$ is summarized in Table 4 with $H^*(10)_{thr.}$ and $H^*(10)_{con.}$, which are the neutron ambient dose equivalents evaluated by the three-group approximation method[4] and our conventional dosemeter[6], respectively. Here, $H^*(10)_{thr.}$ is a more precise value because $H^*(10)_{thr.}$ was evaluated by multiplying the neutron fluence-to-ambient dose equivalent conversion factor and the neutron spectrum unfolding using the three-group approximation method. Therefore, the relative errors $\varepsilon_{con.}$ and $\varepsilon_{exp.}$ were calculated by comparing $H^*(10)_{con.}$ and $H^*(10)_{exp.}$ with $H^*(10)_{thr.}$, which is the reference value. The value of $\varepsilon_{exp.}$ decreased to ∼30% compared with the value of $\varepsilon_{con.}$, which was ∼50%. As mentioned above in Section Confirmation of the Validity of the Present Method, the response of the present dosemeter was not improved in the epithermal region compared with our conventional dosemeter, whereas it was improved in the fast-neutron region. This decrease of $\varepsilon_{exp.}$ was the successful result from the improvement of the response of the present dosemeter in the fast-neutron region. From these results, we found that the present double neutron dosemeter system, which evaluates slow- and fast-neutrons separately, was useful for a more accurate $H^*(10)$ evaluation than our conventional dosemeter using a single CsI scintillator.

In addition, $H^*(10)_{exp.}$ in the experiment conducted around the 10 MV medical Linac was overestimated, whereas all values of $H^*(10)_{sim.}$ estimated through a PHITS simulation conducted at five medical Linacs, the acceleration voltages of which were above 15 MV, were underestimated. Hence, the present neutron dosemeter was suitable for the neutron dosimetry around a Linac with an acceleration voltage of no higher than 10 MV. However, the higher the acceleration voltage is, the larger the number of neutrons produced. Therefore, for the fast-neutron dosemeter, it will be desirable to reach the level of the ICPR-74 rem-response at a higher energy region in the future.

CONCLUSION

The development of a neutron dosemeter using double self-activated CsI detectors was carried out to simply evaluate neutron ambient dose equivalents with a high accuracy. After the design of the neutron dosemeter was optimized, the response of the neutron dosemeter was shown to be in good agreement with the ICRP-74 rem-responses in a wide energy range from a thermal to 3 MeV neutrons, except for the epithermal region. The validity of the present method was confirmed by evaluating the neutron ambient dose equivalents under various Linac conditions using a PHITS simulation and based on experiment results. In the PHITS simulation conducted at Linacs with an acceleration voltage of above 15 MV, the present dosemeter was able to achieve a value of $H^*(10)$ with a precision similar to that of the three-group approximation method, although the value was underestimated. In an experiment conducted around a 10 MV Linac, the present dosemeter was able to evaluate $H^*(10)$ more accurately than our conventional dosemeter. In conclusion, it is expected that the present double neutron dosemeter system can evaluate $H^*(10)$ simply with a high accuracy around a 10 MV Linacs.

ACKNOWLEDGEMENTS

This study was conducted in part under the Cooperative Research at Kindai University Reactor supported by the Graduate School of Engineering, Osaka

University. The authors thank Mr. T. Ueki of the Clinical Support Department, Hiroshima University Hospital, and Mr. R. Kurihara of the High-precision Radiotherapy Center, Hiroshima Heiwa Clinic.

CONFLICT OF INTEREST

The authors declare that they have no conflict of interest.

REFERENCES

1. Wolff, D. *et al. Volumetric modulated arc therapy (VMAT) vs. serial tomotherapy, step-and-shoot IMRT and 3D-conformal RT for treatment of prostate cancer*. Radiother. Oncol. **93**(2), 226–233 (2009).
2. Hall, E. J., Martin, S. G., Amols, H. and Hei, T. K. *Photoneutrons from medical linear accelerators-radiobiological measurements and risk estimates*. Int. J. Radiat. Oncol. Biol. Phys. **33**(1), 225–230 (1995).
3. Wakabayashi, G., Nohtomi, A., Yahiro, E., Fujibuchi, T., Fukunaga, J., Umezu, Y., Nakamura, Y., Nakamura, K., Hosono, M. and Itoh, T. *Applicability of self-activation of an NaI scintillator for measurement of photo-neutrons around a high-energy X-ray radiotherapy machine*. Radiol. Phys. Technol. **8**(1), 125–134 (2015).
4. Kakino, R., Nohtomi, A. and Wakabayashi, G. *Improvement of neutron spectrum unfolding based on three-group approximation using CsI self-activation method for evaluation of neutron dose around medical linacs*. Radiat. Meas. **116**(June), 40–45 (2018).
5. Nohtomi, A., Wakabayashi, G. and Kinoshita, H. *High sensitive neutron-detection by using a self-activation of iodine-containing scintillators for the photo-neutron monitoring around X-ray radiotherapy machines*. JPS Conf. Proc. **11**, 050002 (2016).
6. Ueki, T., Nohtomi, A., Wakabayashi, G., Fukunaga, J., Kato, T. and Ohga, S. *A design study of application of the CsI self-activation method to the neutron rem-counter technique*. Radiat. Meas. **128**(March), 106181 (2019).
7. Nakamura, T., Hara, A. and Suzuki, T. *Realization of a high sensitivity neutron rem counter*. Nucl. Inst. Methods Phys. Res. A. **241**(2–3), 554–560 (1985).
8. Kakino, R. Development of neutron dose evaluation method during radiation therapy by using the self-activation of a CsI scintillator. Master's thesis. (Department of Health Sciences. Kyushu University) (2018).
9. International Commission on Radiation Protection. *Conversion coefficients for use in radiological protection against external radiation*. Int. Comm. Radiolodical. Prot. **26**(12), 7250–7257 (1996).
10. Hamamatsu Photonics. Radiation detection module C12137. Available on https://www.hamamatsu.com/jp/en/product/type/C12137/index.html (accessed January 15, 2020).
11. Sato, T. *et al. Particle and heavy ion transport code system, PHITS, version 2.52*. J. Nucl. Sci. Technol. **50**(9), 913–923 (2013).
12. Yamaguchi, I., Tanaka, S., Fujibuchi, T., Kida, T., Nagaoka, H. and Watanabe, H. *Nationwide survey on the operational status of electron accelerators for radiation therapy in Japan*. Radiol. Phys. Technol. **3**(2), 98–103 (2010).
13. Montgomery, L., Evans, M., Liang, L., Maglieri, R. and Kildea, J. *The effect of the flattening filter on photoneutron production at 10 MV in the Varian TrueBeam linear accelerator*. Med. Phys. **45**(10), 4711–4719 (2018).
14. Uchida, Y. and Saegusa, J. *Characteristics of thermal neutron calibration field using a graphite pile*. JAEA-Tech. , 2005-012 (2005).
15. Yoshizawa, M., Saegusa, J., Tanimura, Y. and Kajimoto, Y. *Calibration fields using RI neutron sources at facility of radiation standards of JAERI*. JAEA-Conf. 2003-002 (2003).
16. Domingo, C. *et al. Neutron spectrometry and determination of neutron ambient dose equivalents in different LINAC radiotherapy rooms*. Radiat. Meas. **45**(10), 1391–1397 (2010).
17. Nohtomi, A. and Wakabayashi, G. *Accuracy of neutron self-activation method with iodine-containing scintillators for quantifying 128I generation using decay-fitting technique*. Nucl. Instrum. Methods Phys. Res. Sect. A. Accel. Spectrometers, Detect. Assoc. Equip. **800**, 6–11 (2015).